

# $\phi$ -Meson Production at RHIC Energies using the PHENIX Detector

Deepali Sharma

for the PHENIX collaboration.

7th October, 2008



# *Outline*

## **1** *Motivation*

## **2** *The PHENIX detector*

## **3** $\phi \rightarrow K^+K^-$ and $\phi \rightarrow e^+e^-$

- $\phi$  spectra
- Yield and Temperature

## **4** *Elliptic flow*

- $v_2$  of Baryons and Mesons
- $v_2$  of  $\phi$

## **5** *Nuclear Modification Factor*

- $R_{dA}$  and  $R_{AA}$

## **6** *Summary*

# Outline

## 1 Motivation

## 2 The PHENIX detector

## 3 $\phi \rightarrow K^+K^-$ and $\phi \rightarrow e^+e^-$

- $\phi$  spectra
- Yield and Temperature

## 4 Elliptic flow

- $v_2$  of Baryons and Mesons
- $v_2$  of  $\phi$

## 5 Nuclear Modification Factor

- $R_{dA}$  and  $R_{AA}$

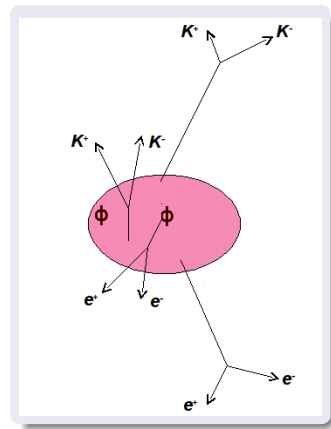
## 6 Summary

# Motivation

$\phi$ -meson, a unique probe

$\phi$  is lightest ( $s\bar{s}$ ) vector meson

- Its production is OZI suppressed in p+p collisions.
- Small cross-section with non-strange hadrons, lifetime  $\tau \sim 46\text{fm}/c$ .
  - carries information from the early partonic stages of the system evolution.
- A diagnostic probe to Chiral Symmetry Restoration that can manifest itself in:
  - line shape(peak position and/or width) modifications.  $\tau_\phi = 46\text{fm}/c, \tau_{QGP} = 10\text{fm}/c \Rightarrow$  only a small fraction of  $\phi$  decays inside the fireball producing a very small modification in the line shape(tail at lower masses).
  - change in the BR of the  $\phi$  decay through  $e^+e^-$  to the  $K^+K^-$  decay channel.
- Comparable in mass to  $\Lambda, p$  baryons, so its  $v_2$  and  $R_{cp}$  provide a critical test for mass or meson/baryon or quark content dependencies and an insight into particle production mechanisms.



PHENIX measures  $\phi$  through both  $e^+e^-$  and  $K^+K^-$  decay channels.

# *Outline*

## 1 *Motivation*

## 2 *The PHENIX detector*

## 3 $\phi \rightarrow K^+K^-$ and $\phi \rightarrow e^+e^-$

- $\phi$  spectra
- Yield and Temperature

## 4 *Elliptic flow*

- $v_2$  of Baryons and Mesons
- $v_2$  of  $\phi$

## 5 *Nuclear Modification Factor*

- $R_{dA}$  and  $R_{AA}$

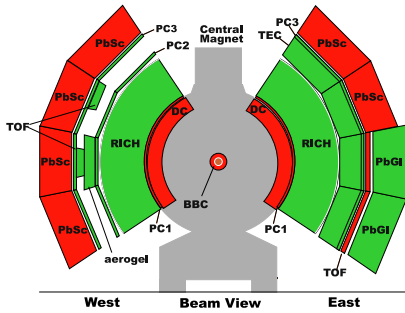
## 6 *Summary*

# The PHENIX detector

PHENIX Central arms Acceptance:

$$-0.35 < \eta < 0.35,$$

$2 \times 90^\circ$  for two arms



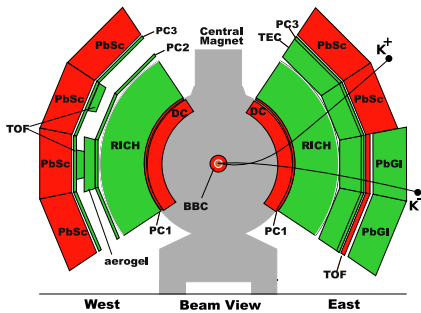
- Vertex: **BBC**
- Tracking: **DC/PC1**
- Matching: **PC3**
- Trigger:
  - Min. bias: **BBC**
  - e: **RICH, EmCal**
- h ID: Time-of-flight
  - **TOF**  $d\tau \sim 100$  ns
  - **EmCal**  $d\tau \sim 500$  ns
  - **Aerogel**  $d\tau \sim 500$  ns
- e ID:
  - Čerenkov light **RICH** ( $e/\pi$  rejection  $>1000$ )
  - E-p matching **EmCal**  $\sim 10$

# The PHENIX detector

PHENIX Central arms Acceptance:

$$-0.35 < \eta < 0.35,$$

$2 \times 90^\circ$  for two arms



- Vertex: BBC
- Tracking: DC/PC1
- Matching: PC3
- Trigger:
  - Min. bias:BBC
  - e: RICH,EmCal
- h ID: Time-of-flight
  - TOF  $d\tau \sim 100$  ns
  - EmCal  $d\tau \sim 500$  ns
  - Aerogel  $d\tau \sim 500$  ns
- e ID:
  - Čerenkov light RICH( $e/\pi$  rejection >1000)
  - E-p matching EmCal  $\sim 10$

Measured decays of  $\phi$

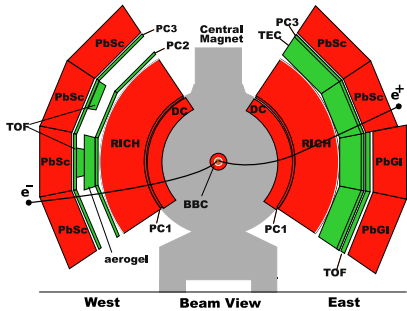
- $\phi \rightarrow K^+ K^-$ : BR =  $49.2 \pm 0.7\%$

# The PHENIX detector

PHENIX Central arms Acceptance:

$$-0.35 < \eta < 0.35,$$

$2 \times 90^\circ$  for two arms



- Vertex: **BBC**
- Tracking: **DC/PC1**
- Matching: **PC3**
- Trigger:
  - Min. bias: **BBC**
  - e: **RICH, EmCal**
- h ID: Time-of-flight
  - **TOF**  $d\tau \sim 100$  ns
  - **EmCal**  $d\tau \sim 500$  ns
  - **Aerogel**  $d\tau \sim 500$  ns
- e ID:
  - Čerenkov light **RICH** ( $e/\pi$  rejection  $>1000$ )
  - E-p matching **EmCal**  $\sim 10$

Measured decays of  $\phi$

- $\phi \rightarrow K^+ K^-$ : **BR** =  $49.2 \pm 0.7\%$
- $\phi \rightarrow e^+ e^-$ : **BR** =  $(2.97 \pm 0.04) \times 10^{-4}$

# Outline

## 1 Motivation

## 2 The PHENIX detector

## 3 $\phi \rightarrow K^+K^-$ and $\phi \rightarrow e^+e^-$

- $\phi$  spectra
- Yield and Temperature

## 4 Elliptic flow

- $v_2$  of Baryons and Mesons
- $v_2$  of  $\phi$

## 5 Nuclear Modification Factor

- $R_{dA}$  and  $R_{AA}$

## 6 Summary

$\phi \rightarrow K^+K^-$  *and*  $\phi \rightarrow e^+e^-$

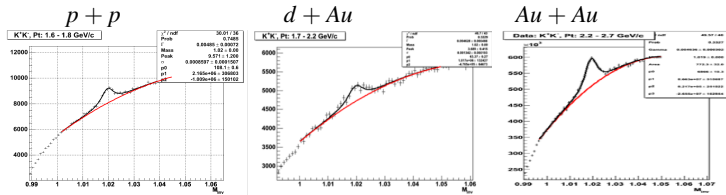
$\phi \rightarrow K^+K^-$  measured using two methods       $\phi \rightarrow e^+e^-$

- No Kaon identification
- One Kaon identified

$\phi \rightarrow K^+K^-$  and  $\phi \rightarrow e^+e^-$

$\phi \rightarrow K^+K^-$ ,  $\sqrt{s_{NN}} = 200$  GeV)

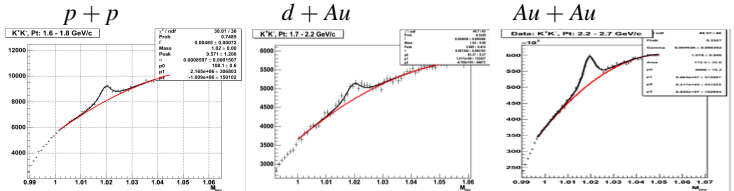
## No Kaon ID



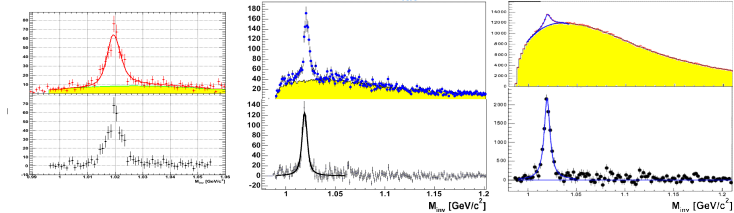
$\phi \rightarrow K^+K^-$  and  $\phi \rightarrow e^+e^-$

$\phi \rightarrow K^+K^-$ ,  $\sqrt{s_{NN}} = 200$  GeV)

## No Kaon ID



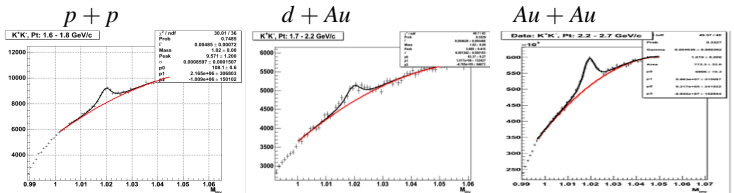
## Two Kaons ID



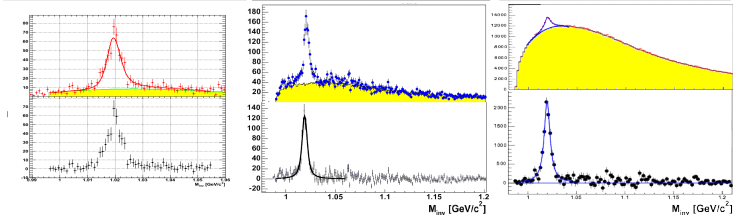
$\phi \rightarrow K^+K^-$  and  $\phi \rightarrow e^+e^-$

$\phi \rightarrow K^+K^-$ ,  $\sqrt{s_{NN}} = 200$  GeV

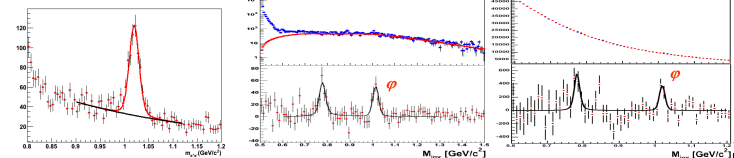
## No Kaon ID



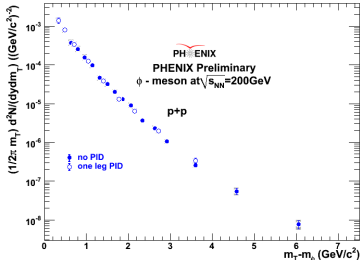
## Two Kaons ID



$\phi \rightarrow e^+e^-$



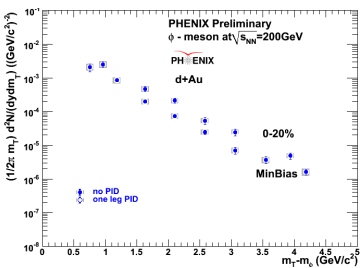
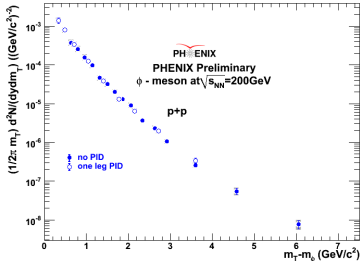
# $\phi \rightarrow K^+K^-$ spectra



## Data Set

- p+p 200 GeV: new Run5 measurements
- d+Au 200 GeV: Run3.
- Au+Au 200 GeV: Run4
- Two independent analyses agree in Au+Au and two in p+p.
- extended  $p_T$  coverage.
- Au+Au 62.4 GeV: Run4

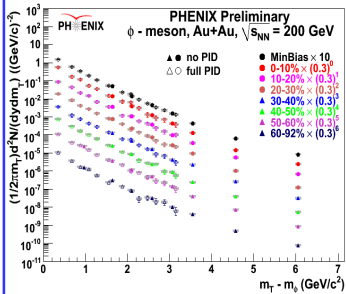
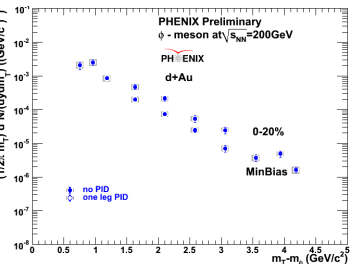
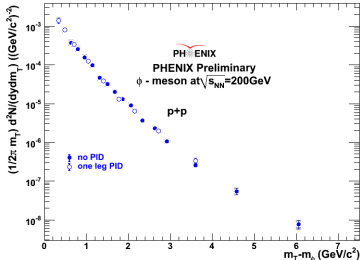
# $\phi \rightarrow K^+K^-$ spectra



## Data Set

- p+p 200 GeV: new Run5 measurements
- d+Au 200 GeV: Run3.
- Au+Au 200 GeV: Run4
- Two independent analyses agree in Au+Au and two in p+p.
- extended  $p_T$  coverage.
- Au+Au 62.4 GeV: Run4

# $\phi \rightarrow K^+K^-$ spectra



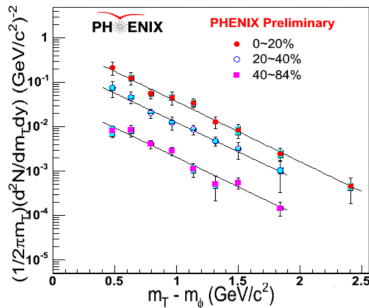
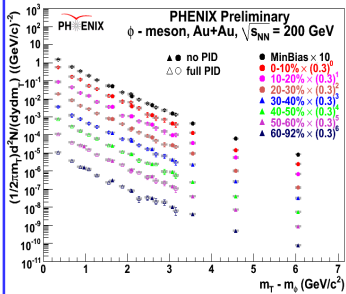
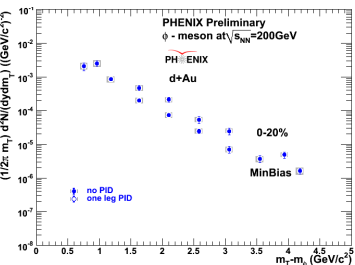
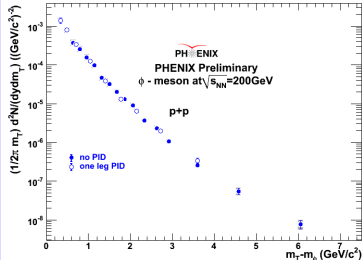
## Data Set

- p+p 200 GeV: new Run5 measurements
- d+Au 200 GeV: Run3.
- Au+Au 200 GeV: Run4

- Two independent analyses agree in Au+Au and two in p+p.
- extended  $p_T$  coverage.

- Au+Au 62.4 GeV: Run4

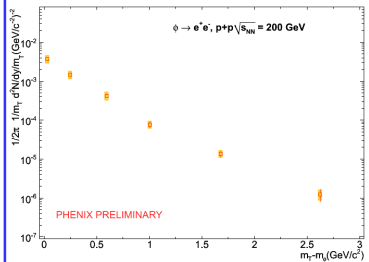
# $\phi \rightarrow K^+K^-$ spectra



## Data Set

- p+p 200 GeV: new Run5 measurements
- d+Au 200 GeV: Run3.
- Au+Au 200 GeV: Run4
- Two independent analyses agree in Au+Au and two in p+p.
- extended  $p_T$  coverage.
- Au+Au 62.4 GeV: Run4

# $\phi \rightarrow e^+e^-$ spectra



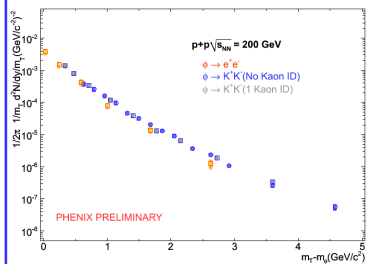
## Data Set

- $p+p$  200 GeV:  
Run5

- $d+Au$  200 GeV:  
Run3

- $Au+Au$  200 GeV:  
Run4

# $\phi \rightarrow e^+e^-$ spectra



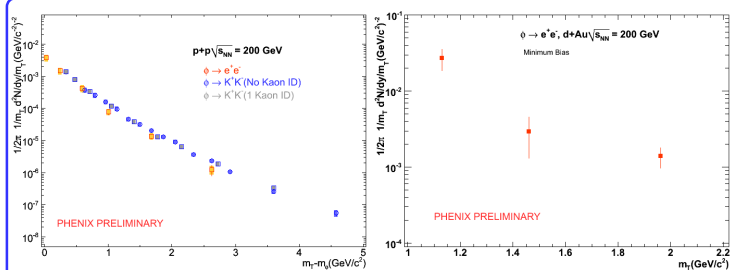
## Data Set

- $p+p$  200 GeV:  
Run5

- $d+Au$  200 GeV:  
Run3

- $Au+Au$  200 GeV:  
Run4

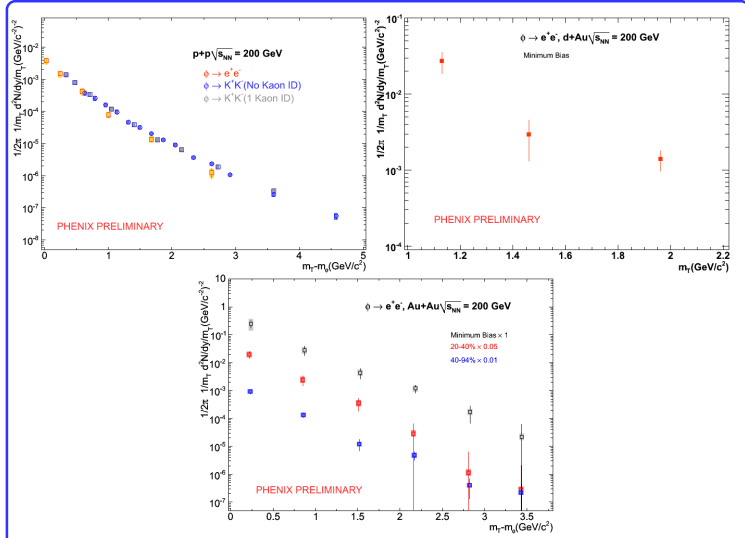
# $\phi \rightarrow e^+e^-$ spectra



## Data Set

- $p+p$  200 GeV:  
Run5
- $d+Au$  200 GeV:  
Run3
- $Au+Au$  200 GeV:  
Run4

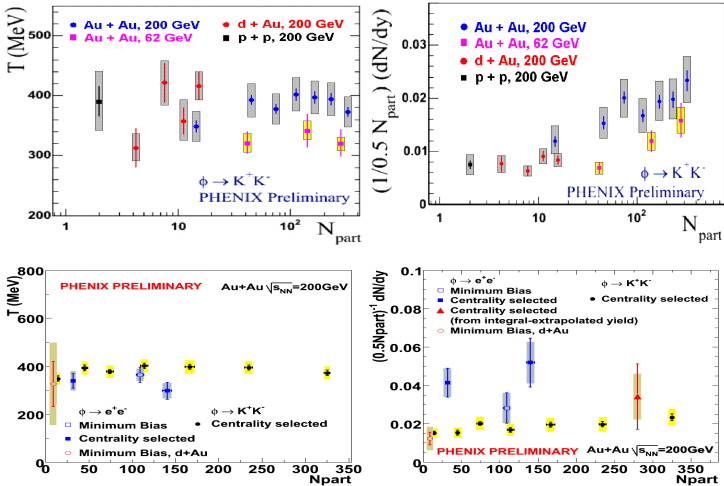
# $\phi \rightarrow e^+e^-$ spectra



## Data Set

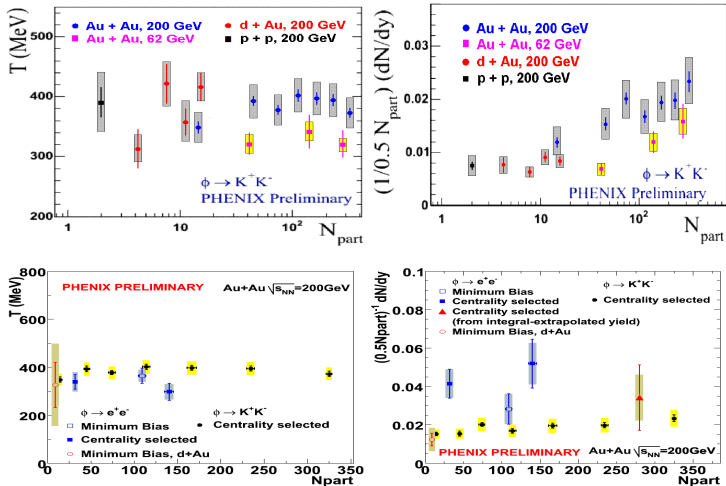
- $p+p$  200 GeV:  
Run5
- $d+Au$  200 GeV:  
Run3
- $\text{Au+Au}$  200 GeV:  
Run4

# $\phi$ -meson yield and temperature



- Temperature  $\sim$  same @ 62, 200 GeV, constant with  $N_{\text{part}}$
- Yield grows with  $\sqrt{s_{\text{NN}}}$  and Centrality.
- Slope measured with leptonic channel is consistent to the Hadronic mode.
- Yield in  $e^+e^-$  channel seems higher, compared to  $K^+K^-$  channel, but errors bars are large to make any conclusive statement.

# $\phi$ -meson yield and temperature



- Temperature  $\sim$  same @ 62, 200 GeV, constant with  $N_{\text{part}}$
- Yield grows with  $\sqrt{s_{\text{NN}}}$  and Centrality.
- Slope measured with leptonic channel is consistent to the Hadronic mode.
- Yield in  $e^+ e^-$  channel seems higher, compared to  $K^+ K^-$  channel, but errors bars are large to make any conclusive statement.

# Outline

## 1 Motivation

## 2 The PHENIX detector

## 3 $\phi \rightarrow K^+K^-$ and $\phi \rightarrow e^+e^-$

- $\phi$  spectra
- Yield and Temperature

## 4 Elliptic flow

- $v_2$  of Baryons and Mesons
- $v_2$  of  $\phi$

## 5 Nuclear Modification Factor

- $R_{dA}$  and  $R_{AA}$

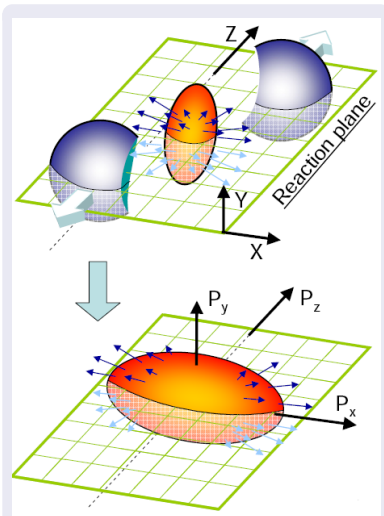
## 6 Summary

# Elliptic Flow

## Elliptic flow $v_2$

- The measured  $v_2$  reflects the dense matter created in the initial stages of heavy-ion collisions.
- $v_2$  is a measure of anisotropy of particles in momentum space, produced during the early stages of heavy-ion collisions. Non-central A+A collisions result in an azimuthal anisotropic distribution in co-ordinate space. Due to pressure gradients and interactions among the particles, the initial space anisotropy gets converted to momentum anisotropy.
- The signal is self quenching  $\Rightarrow$  **early time observable**.
- $v_2$  is the 2<sup>nd</sup> coefficient of an azimuthal Fourier expansion of the transverse momentum spectrum around the beam axis.

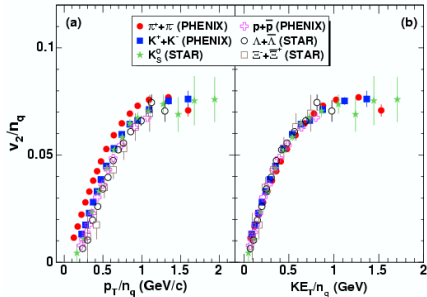
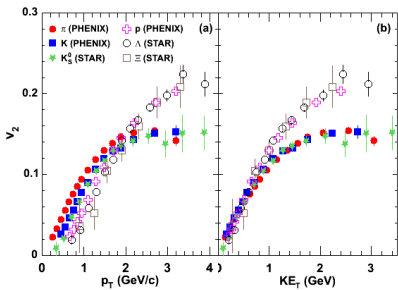
$$E \cdot \frac{d^3N}{dp^3} = \frac{1}{2\pi} \cdot \frac{d^2N}{dp_T dy} \cdot [1 + 2\nu_1 \cos(2\phi) + 2\nu_2 \cos(2\phi) + \dots]$$
$$\nu_2 = \langle \cos(2\phi) \rangle$$



## *v*<sub>2</sub> of Baryons and Mesons

$\pi$ , K, p (PHENIX) PRL 98, 162301 (2007)

$K^0_s$ ,  $\Lambda$  (STAR): PRL 92, 052302 (2004)  $\Xi$  (STAR): PRL 95, 122301 (2005)

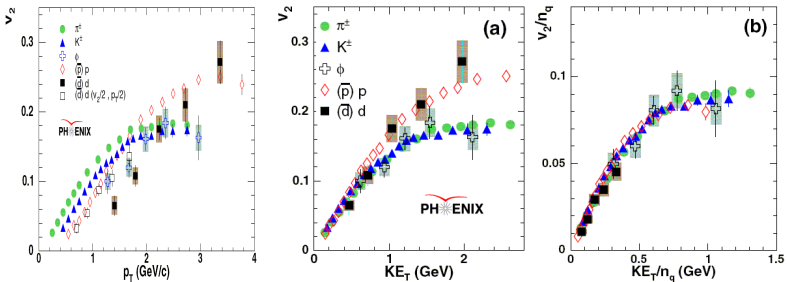


- At low transverse momentum ( $p_T \leq 2.0$  GeV/c),  $v_2$  is consistent with the mass ordering expected from hydrodynamics.
- Results are consistent with Quark number + $KE_T$  scaling.

- The systematic measurements of  $v_2$  for the strange hadrons  $\Lambda$ ,  $K_s^0$ ,  $\Xi$  and  $\Omega$  suggest that collectivity is developed at the partonic stage at RHIC.
- This concept of partonic collectivity can further be strengthened if  $\phi$ -meson flows like the other mesons.

$v_2$  of  $\phi$

Au+Au  $\sqrt{s_{NN}}=200\text{GeV}$



Phys. Rev. Lett. 99, 052301 (2007)

- $\phi$ -meson shows a significant flow, with a similar trend as that  $\pi^\pm$  and  $K^\pm$  at higher  $p_T$ 
  - consistent with universal scaling of  $v_2$  per constituent quarks.
  - flow is developed at the partonic level at RHIC.
- $\phi$  is created via coalescence of thermalized quarks in Au+Au

# Outline

## 1 Motivation

## 2 The PHENIX detector

## 3 $\phi \rightarrow K^+K^-$ and $\phi \rightarrow e^+e^-$

- $\phi$  spectra
- Yield and Temperature

## 4 Elliptic flow

- $v_2$  of Baryons and Mesons
- $v_2$  of  $\phi$

## 5 Nuclear Modification Factor

- $R_{dA}$  and  $R_{AA}$

## 6 Summary

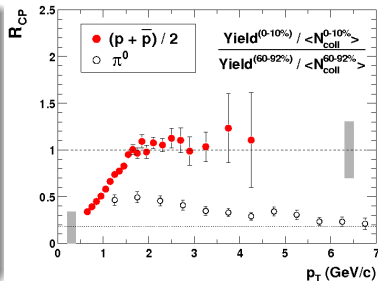
# Nuclear Modification Factor

The nuclear Modification factor  $R_{AA}$  is

$$R_{AA}(p_T) = \frac{d^2N^{AA}/dp_Tdy}{\langle n_{coll} \rangle \cdot d^2N^{pp}/dp_Tdy}$$

$R_{cp}$  is the ratio of central to peripheral yields scaled by their respective  $N_{coll}$  value.

$$R_{CP}(p_T) = \frac{N_{coll}^{peripheral}}{N_{coll}^{central}} \cdot \frac{d^2N_{AA}^C/dp_Tdy}{d^2N_{AA}^P/dp_Tdy}$$



Phys. Rev. Lett 91, 172301 (2003)

- Pions are suppressed in Central Au+Au collisions @ 200 GeV
- Protons show no suppression at 2-4 GeV/c.
- The suppression pattern depends on particle species.

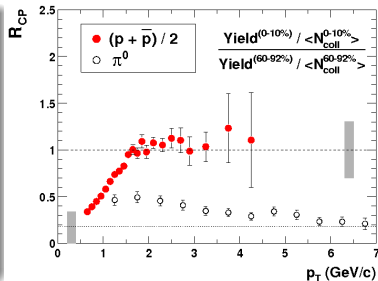
Systematic measurements of  $R_{AA}$  and  $R_{CP}$  for various particles helps to understand the nuclear medium effects on hadron production.

The nuclear Modification factor  $R_{AA}$  is

$$R_{AA}(p_T) = \frac{d^2N^{AA}/dp_Tdy}{\langle n_{coll} \rangle \cdot d^2N^{pp}/dp_Tdy}$$

$R_{cp}$  is the ratio of central to peripheral yields scaled by their respective  $N_{coll}$  value.

$$R_{CP}(p_T) = \frac{N_{coll}^{peripheral}}{N_{coll}^{central}} \cdot \frac{d^2N_{AA}^C/dp_Tdy}{d^2N_{AA}^P/dp_Tdy}$$



Phys. Rev. Lett 91, 172301 (2003)

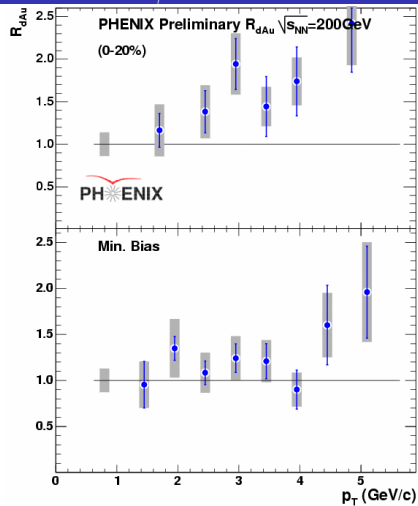
- Pions are suppressed in Central Au+Au collisions @ 200 GeV
- Protons show no suppression at 2-4 GeV/c.
- The suppression pattern depends on particle species.

**Systematic measurements of  $R_{AA}$  and  $R_{CP}$  for various particles helps to understand the nuclear medium effects on hadron production.**

# $\phi$ -Nuclear modification factor

in d+Au 200 GeV

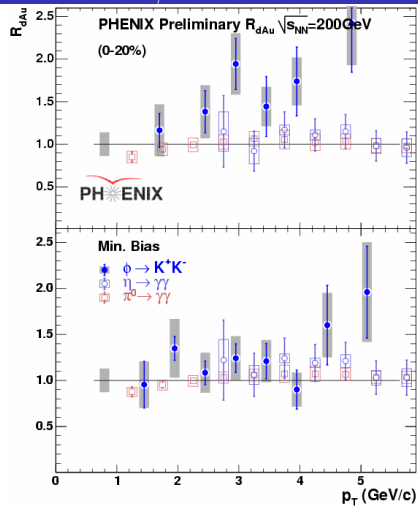
$$\phi \rightarrow K^+ K^-$$



# $\phi$ -Nuclear modification factor

in d+Au 200 GeV

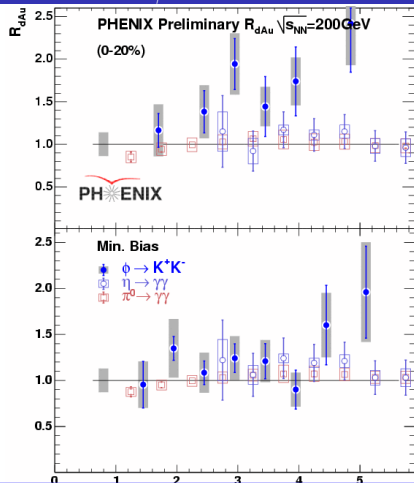
$$\phi \rightarrow K^+ K^-$$



# $\phi$ -Nuclear modification factor

in d+Au 200 GeV

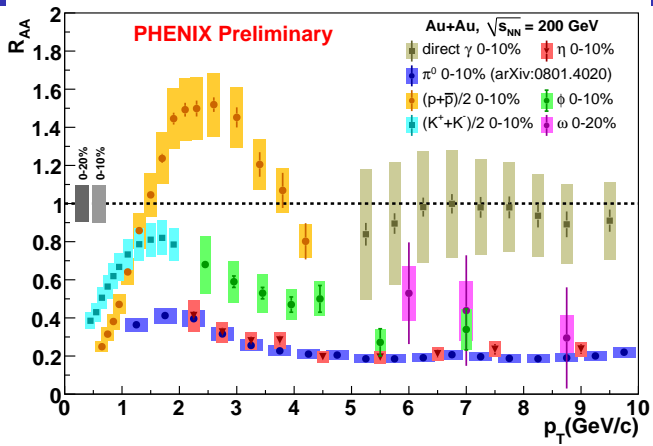
$$\phi \rightarrow K^+ K^-$$



- $\phi$  is not suppressed in d+Au
- $R_{dA}$  of  $\pi^0$ ,  $\eta$  is consistent with 1.  $\phi$  enhancement in 0-20%?
- Large error bars leave some room for Cronin enhancement

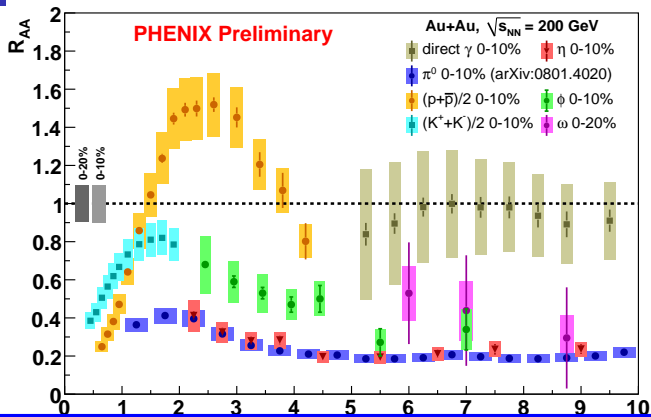
# $\phi$ -Nuclear modification factor

in Au+Au 200 GeV



# $\phi$ -Nuclear modification factor

in Au+Au 200 GeV

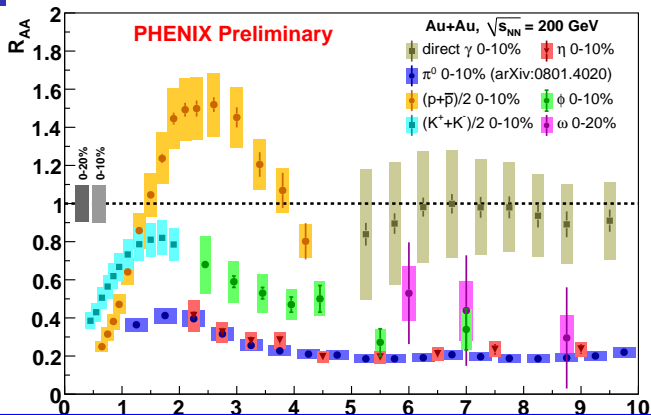


The known fact:

Hadron suppression patterns do not depend on the mass of the particles, but they are sensitive to the number of valence quarks.

# $\phi$ -Nuclear modification factor

in Au+Au 200 GeV



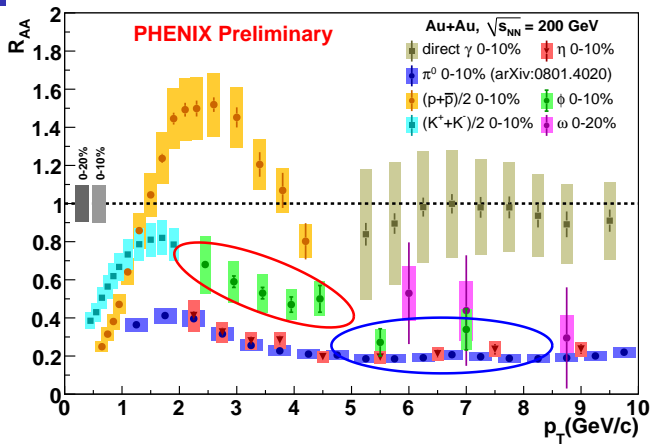
The known fact:

Hadron suppression patterns do not depend on the mass of the particles, but they are sensitive to the number of valence quarks.

$\phi$  meson does not fit into common picture...  
 It is less suppressed than  $\pi^0$  and  $\eta$  at intermediate  $p_T$ .  
 Does suppression depend on quark flavor composition?

# $\phi$ -Nuclear modification factor

in Au+Au 200 GeV



At high  $p_T$ : the  $\phi$ - suppression level is similar to that of  $\eta$  and  $\pi^0$

At Intermediate  $p_T$ : the suppression pattern is different.

# Outline

## 1 Motivation

## 2 The PHENIX detector

## 3 $\phi \rightarrow K^+K^-$ and $\phi \rightarrow e^+e^-$

- $\phi$  spectra
- Yield and Temperature

## 4 Elliptic flow

- $v_2$  of Baryons and Mesons
- $v_2$  of  $\phi$

## 5 Nuclear Modification Factor

- $R_{dA}$  and  $R_{AA}$

## 6 Summary

## Summary

PHENIX has measured  $\phi$ -meson in  $p + p$ ,  $d + Au$  and  $Au + Au$  collisions  $\sqrt{s_{NN}} = 200\text{GeV}$  by  $K^+K^-$  and  $e^+e^-$  decay modes.

The measurements using  $K^+K^-$  decay channels are complete in all systems. The leptonic channel measurement suffer due to combinatorial background and statistics in  $Au + Au$  and  $d + Au$ .

The measurements using  $K^+K^-$  channel are extended to higher  $p_T$  in  $p + p$  and  $Au + Au$ .

The  $\phi v_2$  is consistent with other mesons and follows Quark number  $+KE_T$  scaling.

In  $d + Au$ , no suppression is seen, but large error bars make room for Cronin enhancement.

The  $R_{AA}$  of  $\phi$ -meson in  $Au + Au$  shows similar suppression pattern to that of  $\pi^0$  and  $\eta$  at high  $p_T$ , but at intermediate  $p_T$ , the suppression pattern is different.

**does quark flavour plays a role ?**

Universidade de São Paulo, Instituto de Física, Caixa Postal 66318, São Paulo CEP05315-970, Brazil  
Institute of Physics, Academia Sinica, Taipei 11529, Taiwan  
China Institute of Atomic Energy (CIAE), Beijing, People's Republic of China  
Peking University, Beijing, People's Republic of China  
Charles University, Ovocnytrh 5, Praha 1, 116 36, Prague, Czech Republic  
Czech Technical University, Zikova 4, 166 36 Prague 6, Czech Republic  
Institute of Physics, Academy of Sciences of the Czech Republic, Na Slovance 2,  
182 21 Prag 8, Czech Republic

Helsinki Institute of Physics and University of Jyväskylä, P.O.Box 35, FI-40014 Jyväskylä, Finland  
Dapnia, CEA Saclay, F-91191 Gif-sur-Yvette, France  
Laboratoire Leprince-Ringuet, Ecole Polytechnique, CNRS-IN2P3, Route de Saclay,  
F-91128, Palaiseau, France

Laboratoire de Physique Corpusculaire (LPC), Université Blaise Pascal, CNRS-IN2P3,  
Clermont-Fd, 63177 Aubière Cedex, France  
IPN-Orsay, Université Paris Sud, CNRS-IN2P3, BP1, F-91406, Orsay, France  
SUBATECH (Ecole des Mines de Nantes, CNRS-IN2P3, Université de Nantes)  
BP 20722 - 44307, Nantes, France

Institut für Kemphysik, University of Münster, D-48149 Münster, Germany  
Debrecen University, H-4010 Debrecen, Egyetem tér 1, Hungary  
ELTE, Eötvös Loránd University, H - 1117 Budapest, Pázmány P. s. 1/A, Hungary  
KFKI Research Institute for Particle and Nuclear Physics of the Hungarian Academy of Sciences (MTA KFKI RMKI),  
H-1525 Budapest 114, POBox 49, Budapest, Hungary

Department of Physics, Banaras Hindu University, Varanasi 221005, India

Bhabha Atomic Research Centre, Bombay 400 085, India  
Weizmann Institute, Rehovot 76100, Israel

Center for Nuclear Study, Graduate School of Science, University of Tokyo, 7-3-1 Hongo, Bunkyo,  
Tokyo 113-0033, Japan

Hirosshima University, Kagamiyama, Higashi-Hiroshima 739-8526, Japan

KEK, High Energy Accelerator Research Organization, Tsukuba, Ibaraki 305-0801, Japan

Kyoto University, Kyoto 606-8502, Japan

Nagasaki Institute of Applied Science, Nagasaki-shi, Nagasaki 851-0193, Japan

RIKEN, The Institute of Physical and Chemical Research, Wako, Saitama 351-0198, Japan

Physics Department, Rikkyo University, 3-34-1 Nishi-Ikebukuro, Toshima, Tokyo 171-8501, Japan

Department of Physics, Tokyo Institute of Technology, Oh-okayama, Meguro, Tokyo 152-8551, Japan

Institute of Physics, University of Tsukuba, Tsukuba, Ibaraki 305, Japan

Waseda University, Advanced Research Institute for Science and Engineering, 17 Kikui-cho,  
Shinjuku-ku, Tokyo 162-0044, Japan

Chonbuk National University, Jeonju, Korea

Ewha Womans University, Seoul 120-750, Korea

KAERI, Cyclotron Application Laboratory, Seoul, South Korea

Kangnung National University, Kangnung 210-702, South Korea

Korea University, Seoul, 136-701, Korea

Myongji University, Yongin, Kyonggi-do 449-728, Korea

System Electronics Laboratory, Seoul National University, Seoul, South Korea

Yonsei University, IPAP, Seoul 120-749, Korea

IHEP Protvino, State Research Center of Russian Federation, Institute for High Energy Physics,  
Protvino, 142281, Russia

Joint Institute for Nuclear Research, 141980 Dubna, Moscow Region, Russia

Russian Research Center "Kurchatov Institute", Moscow, Russia

PNPI, Petersburg Nuclear Physics Institute, Gatchina, Leningrad region, 188300, Russia

Saint Petersburg State Polytechnic University, St. Petersburg, Russia

Skobeltsyn Institute of Nuclear Physics, Lomonosov Moscow State University, Vorob'evy Gory,  
Moscow 119992, Russia

Department of Physics, Lund University, Box 118, SE-221 00 Lund, Sweden



14 Countries; 69 Institutions



July 2007

Abilene Christian University, Abilene, TX 79699, U.S.

Collider-Accelerator Department, Brookhaven National Laboratory, Upton, NY 11973-5000, U.S.

Physics Department, Brookhaven National Laboratory, Upton, NY 11973-5000, U.S.

University of California - Riverside, Riverside, CA 92521, U.S.

University of Colorado, Boulder, CO 80309, U.S.

Columbia University, New York, NY 10027 and Nevis Laboratories, Irvington, NY 10533, U.S.

Florida Institute of Technology, Melbourne, FL 32901, U.S.

Florida State University, Tallahassee, FL 32306, U.S.

Georgia State University, Atlanta, GA 30303, U.S.

University of Illinois at Urbana-Champaign, Urbana, IL 61801, U.S.

Iowa State University, Ames, IA 50011, U.S.

Lawrence Livermore National Laboratory, Livermore, CA 94550, U.S.

Los Alamos National Laboratory, Los Alamos, NM 87545, U.S.

University of Maryland, College Park, MD 20742, U.S.

Department of Physics, University of Massachusetts, Amherst, MA 01003-9337, U.S.

Muhlenberg College, Allentown, PA 18104-5586, U.S.

University of New Mexico, Albuquerque, NM 87131, U.S.

New Mexico State University, Las Cruces, NM 88003, U.S.

Oak Ridge National Laboratory, Oak Ridge, TN 37831, U.S.

RIKEN BNL Research Center, Brookhaven National Laboratory, Upton, NY 11973-5000, U.S.

Chemistry Department, Stony Brook University, Stony Brook, SUNY, NY 11794-3400, U.S.

Department of Physics and Astronomy, Stony Brook University, SUNY, Stony Brook, NY 11794, U.S.

University of Tennessee, Knoxville, TN 37996, U.S.

Vanderbilt University, Nashville, TN 37235, U.S.

# Back ups

$\phi \rightarrow K^+K^-$  spectra

